

CONTRACT NUMBER 508830

DEISA
**DISTRIBUTED EUROPEAN INFRASTRUCTURE FOR
SUPERCOMPUTING APPLICATIONS**

European Community Sixth Framework Programme
RESEARCH INFRASTRUCTURES
Integrated Infrastructure Initiative

Production operation of distributed simulation codes: status
report — second set of projects.

Deliverable ID: DEISA-D-JRA6-5
Due date: October 31st, 2006
Actual delivery date: November 24, 2006
Lead contractor for this deliverable: IDRIS / CNRS, France

Project start date: May 1st, 2004
Duration: 4 years

Project co-funded by the European Commission within the Sixth Framework Programme (2002-2006)		
Dissemination Level		
PU	Public	X
PP	Restricted to other programme participants (including the Commission Services)	
RE	Restricted to a group specified by the consortium (including the Commission	
CO	Confidential, only for members of the consortium (including the Commission Services)	

Table of Content

Table of Content.....	1
1. Introduction.....	2
1.1 Executive Summary.....	2
2. Natural convection / radiation project.....	3
2.1 Coupled 2D numerical simulations.....	3
2.1.1 2D coupling at high Rayleigh number.....	3
2.1.2 Coupling frequency.....	5
2.2 3D coupled application.....	6
2.2.1 Convection code description (NS3D).....	6
2.2.2 Radiative code description (RadMC3D).....	6
2.2.3 3D coupling description.....	7
2.2.4 Migration on the DEISA infrastructure and first improvements.....	7
2.3 Conclusion and future works.....	8
3. FOCUS project.....	9
3.1 Technical Improvement.....	9
3.2 Gas turbine injector simulation.....	9
3.3 Conclusion and future work.....	12
4. The KOP3D project.....	14
4.1 Current scientific usage of KOP3D.....	14
4.2 Necessary parallelization efforts.....	14
4.3 Considerations on shared memory usage with OpenMP.....	15
4.4 Parallel operation and load balancing concepts.....	15
4.4.1 Test case with structured domains.....	16
4.4.2 Test case with unstructured mesh surrounded by structured meshes.....	16
4.5 Load balancing analyses.....	17
4.6 Conclusion and future work.....	19
5. Conclusion.....	20
6. References and Applicable Documents.....	21
7. Document Amendment Procedure.....	23
8. List of Acronyms and Abbreviations.....	24

1. Introduction

1.1 *Executive Summary*

The main objective of JRA6 is to facilitate scientific research projects based on coupling methodology in the DEISA context.

At the project beginning, this JRA dealt with 3 projects called *initial projects* and had reported about their main achievements in D-JRA6-1 [11], D-JRA6-2 [12] and D-JRA6-3 [13] deliverables. In particular, we describe the scientific project and the main objectives for each of them. We explain also how the coupled applications have been migrated and the main technical enhancements made for each coupling project. After exploiting the 3 coupled codes and producing the first numerical results, we highlight the added value on the scientific and technical aspects in this JRA context.

Three new projects, called the *second set*, started 12 months ago. In D-JRA6-4 [14] we introduced these second set projects and reported on the first month activities.

In this document, we mainly complete the scientific description and objectives of these new projects, describe the technical improvements in the second releases and report on their production status.

This document is public.

2. Natural convection / radiation project

<i>Title</i>	Coupling of turbulent natural convection with radiative heat transfer in buildings
<i>Scientific leader</i>	Shihe XIN, LIMSI-CNRS (Laboratoire d'Informatique pour la Mécanique et les Sciences de l'Ingénieur), Orsay, France.
<i>Partner Laboratories</i>	LET (Laboratoire d'Etudes Thermiques), Poitiers, France. EM2C (Laboratoire d'Energetique Moléculaire et Mascroscopique, Combustion), <i>Radiative Transfer team</i> , Chatenay Malabry, France.
<i>Links with other scientific projects</i>	COCORAPHA (COuplage CONvection-RAYonnement Pour l'HABitat) - ACI Energie (Action Concertée Initiative) – funded by the French Ministry of Research.

Before we start to describe our activity during the previous six months, we would like to explain the context of this research activity.

Since seventies, the energy and its usage by mankind have systematically been placed in the heart of events and have progressively become a major geo-politic, economic and societal issue. In 2002, proposed by its Department of Engineering Sciences (DES), the National Center for Scientific Research in France (CNRS) launched the *Energy Program*. This Interdisciplinary Program had 4 major research axes: novel energy resources, energy carriers management, environment and socio-economic impact. Preliminary reports already pointed out the importance of heating consumption for residential and tertiary sectors (60 Mtoe — just after transportation fuel consumption 90 Mtoe). The research work led by the French laboratories LIMSI, LET, EM2C, LEPTAB, LETEM, ... is directly connected with the major topics identified by the *Energy Program*. More recently these laboratories were involved in COCORAPHA (funded by the French Ministry of Research) project to develop and validate a coupled approach.

2.1 Coupled 2D numerical simulations

In the previous deliverable [14] we described the first results of the 2D coupled application. First, we numerically validated the whole coupled application for a square cavity. Then, we showed at a moderate Rayleigh number ($R_a = 10^6$) that the flow behavior (the temperature stratification is weaker and the horizontal velocity is more important near walls) has been slightly modified if one takes account of radiative properties of the gas (air) inside the cavity (this gas is often referenced as the *participating media*).

The last six months were dedicated to investigate different configurations which will serve as reference results for the community and will provide precious information for the first runs of the 3D coupled application.

2.1.1 2D coupling at high Rayleigh number

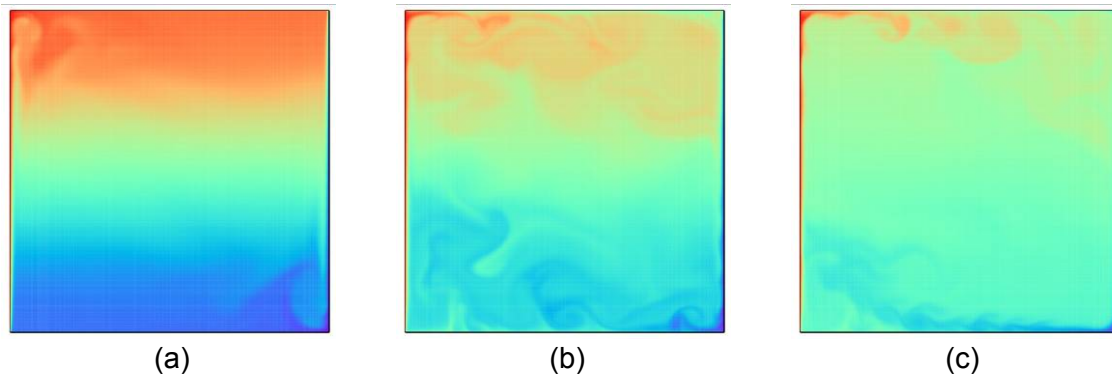
For this new case, we consider a 1 meter high square cavity filled with air. A 10 K temperature difference (exactly $\Delta T = 9.2336$ K) is maintained between the 2 vertical walls. These physical characteristics lead to a high Rayleigh number ($R_a = 10^9$). For this value, a high space and time resolution is required (300 x 300 cells for space resolution and the time step is fixed with the CFL condition).

Figure 1 shows temperature fields which correspond to the following 3 different cases:

- No Radiation Heat Transfer (RHT) phenomenon is considered neither for walls nor for the cavity gas (emissivity $\varepsilon = 0$ and $\kappa = 0$).
- Only the walls are involved in the RHT (emissivity $\varepsilon = 0.5$ and $\kappa = 0 \text{ m}^{-1}$).
- Both the walls and the cavity gas are considered in the RHT processes (emissivity $\varepsilon = 0.5$ and $\kappa = 1 \text{ m}^{-1}$).

only the two last ones correspond to coupled convection/radiation simulations.

Instantaneous Temperature fields



Temperature mean fields

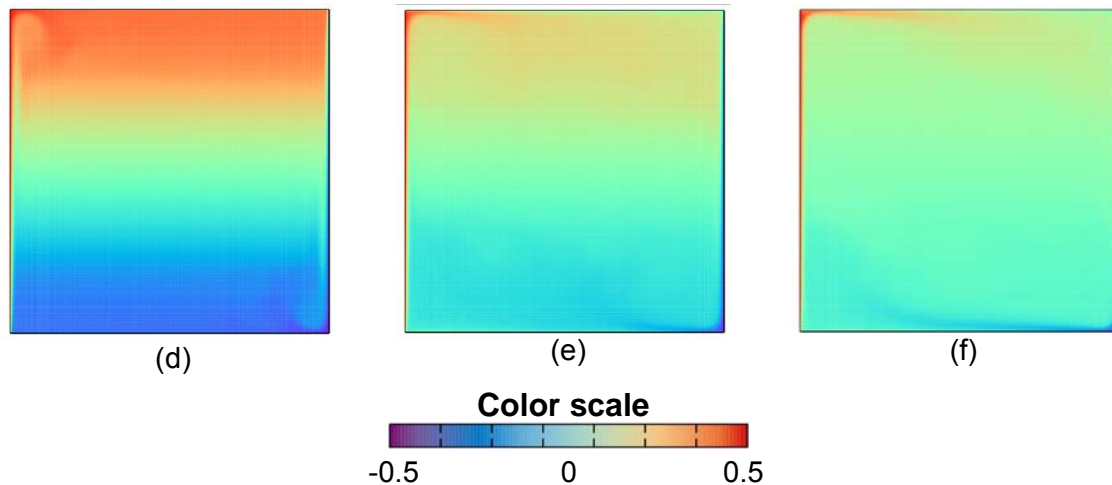


Figure 1: The instantaneous temperature fields (upper images) and the temperature mean fields (lower images) inside an air-filled cavity are represented here for a high Rayleigh number ($R_a = 10^9$). The cases (a) and (d) correspond to a situation without RHT ($\varepsilon = 0$ and $\kappa = 0 \text{ m}^{-1}$). Only the wall RHT is considered ($\varepsilon = 0.5$ and $\kappa = 0 \text{ m}^{-1}$) in the cases (b) and (e). The cases (c) and (f) correspond to a situation where the RHT of both walls and cavity fluid are considered ($\varepsilon = 0.5$ and $\kappa = 1 \text{ m}^{-1}$)

As expected, the coupled simulations (see Figure 1 (b) (e) and (c) (f)) present important differences (compared with lower Rayleigh $R_a = 10^6$ – see [14]) with respect to the pure convection case (see Figure 1 (a) and (d)). Coupling with RHT phenomenon decreases the thermal stratification (see Figure 1 (b) and (e)) and even seems to take off the temperature gradient (see Figure 1 (c) and (f)). More especially RHT processes associated with vertical walls ($\varepsilon = 0.5$) generates important disturbances which spread out near horizontal walls. These turbulences, which mix the cavity gas, seem to be at the

origin of the thermal stratification decreasing. Taking account of both air and wall in the RHT processes seems to decrease slightly the turbulences observed previously and increases the velocity along vertical walls.

As a result, we can conclude that at high Rayleigh number the radiation heat transfer strongly impacts on the flow structure inside the cavity.

2.1.2 Coupling frequency

We have performed numerous coupled simulations for the above-mentioned two RHT situations ($\varepsilon = 0.5$, $\kappa = 0 \text{ m}^{-1}$ and $\varepsilon = 0.5$, $\kappa = 1 \text{ m}^{-1}$) and with different coupling frequencies (from $f = 1$ to $f = 1000$, i.e. from one coupling every time step in the Navier-Stokes code to one coupling every 1000 time steps). The results obtained show that the temperature and velocity fields present small fluctuations for the frequency lower than 150.

In Figure 2 we have selected a small number of case (here 3) among those evoked before. We present in particular the mean temperature fields and the RMS fields obtained with different coupling frequencies when both walls and cavity fluid are involved in the RHT model. Lower coupling frequency cases compared with the one which couples at every time step ($f=1$) show slight modifications in the $f=150$ case and a drastic behavior in the $f = 1000$ case. For this coupling frequency $f=1000$, temperatures are higher along the top horizontal wall (at the opposite temperatures are lower along the bottom horizontal wall) and RMS field presents important fluctuations greater than 3×10^{-3} .

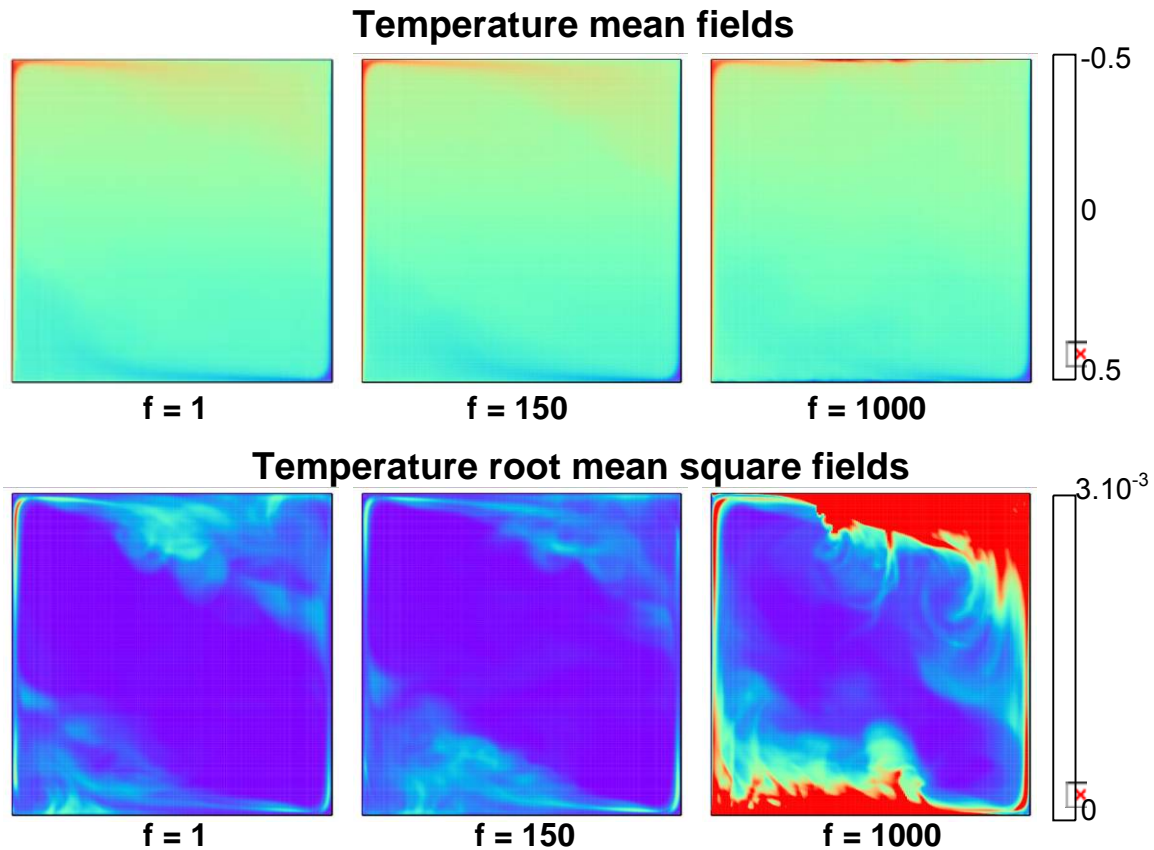


Figure 2: Mean temperature fields (upper fields) and RMS for the RHT model which takes account of both walls and cavity air. Different fields are presented for the following coupling frequencies (f): 1, 150 and 1000.

More detailed investigations must be done to identify the suitable frequency domain to couple convection code with RHT code. In particular, since the fluid behavior is rather turbulent, more statistics must be provided to validate this study.

2.2 **3D coupled application**

In the following we are going to mainly present the radiative code (RadMC3D) and the coupling layer occurring in this new 3D application. Then we are going to describe the work done to adapt the coupled 3D codes on the DEISA infrastructure.

2.2.1 *Convection code description (NS3D)*

In this sub-section we will just sum up the 3D code (called NS3D) description already given in the previous deliverable [14].

In the scope of second-order time scheme and projection method, the resulting Helmholtz equations (for velocity and temperature) and the pseudo-Poisson equation (for pressure) are used to solve the unsteady Navier-stokes equations in the 3D cavity. The parallelism aspects are treated in two steps: in the first each sub-domain solves locally the equations, and then in the second time other sub-domains are considered by using the numerical technique of Shur complement.

2.2.2 *Radiative code description (RadMC3D)*

Calculation of radiative flux and sources in participating media (like ambient air with small concentrations of CO₂ and water vapor) may be seen mainly in two different ways (see [21] and [22]). The first one leads to methods such as the Discrete Ordinates method (DOM) or Multiflux method, which generate approximate solutions to the Radiative Transfer Equation (RTE). The second one consists in solving the RTE with the well-known statistical approach: the Monte Carlo method (MC). Although this method is very time consuming (it requires a lot of iterations), MC method is largely used to give accurate results which serve as reference.

The main ideas about MC method are quite simple. The photon or photon bundle propagation in radiative transfer is viewed as a sequence of elementary events; the main events are the absorption, the emission in the participating media and the reflection on the walls. In the algorithm, the sequence characteristics are chosen randomly: photon wavelength (in adequacy with gas properties inside the cavity), space direction, and the absorption length (depending on participating media properties – for more information see [23], [24] and [25]).

First, the total radiative power emitted by the medium (CO₂ and H₂O in ambient air) and the cavity walls is computed. This energy magnitude depends on the temperature, the composition of the cavity fluid, the spectral absorption coefficient of the medium and the emissivity of the walls.

In a second time, the photon bundle propagation occurs inside the cavity up to the photon bundle absorption by the medium or by the wall (the bundle is indivisible – here, its energy does not decrease gradually). A lot of random sequences are needed to provide accurate results of the radiative power absorbed (typically ten millions of shootings are required for one thousand of mesh boxes). Finally one can compute the total radiative power in the whole cavity – this quantity will be required by the convection code NS3D.

The code RadMC3D has been developed by the team *Radiative Transfer* of the EM2C laboratory especially for this 3D coupling project. This work has been validated during the 6-months period.

2.2.3 3D coupling description

The coupling has been structured with the following features:

- The NS3D code requires (for the case of a cubic cavity) a higher resolution than those needed by the RHT code.
- The RadMC3D mesh is obtained directly by selecting a coarser subset the NS3D one. This means that an interpolation is performed in the coupling part called *adaptor* (see previous deliverable [14]).
- Since the two codes compute in different unit systems (NS3D is dimensionless and RayMC3D used international units) the *adaptor* layer deals with converting these units.

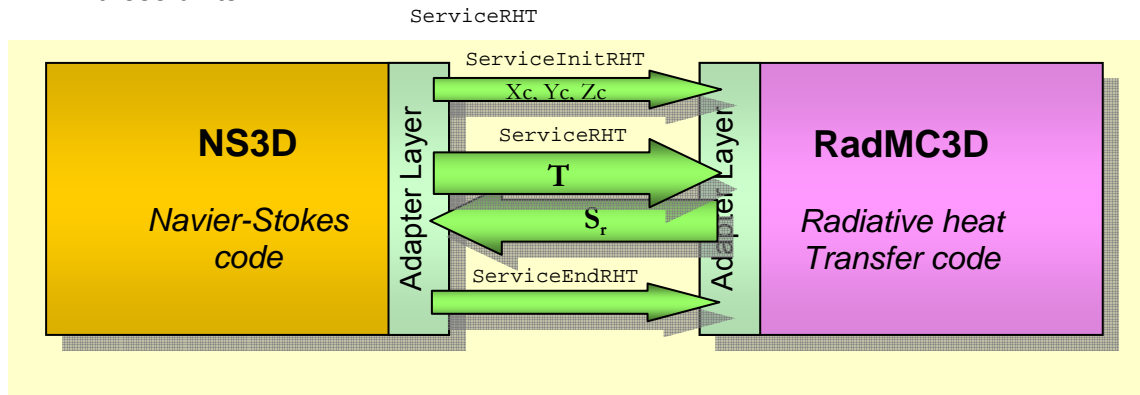


Figure 3: Coupling diagram between the Navier-Stokes code NS3D and the radiative heat transfer called RadMC3D.

Finally, we have globally the same coupling architecture (see Figure 3) than for the 2D case. The main remote call (or service) gives the temperature field (beforehand interpolated in the NS3D adaptor layer) to the RadMC3D code which returns the radiative power (at its turn the radiative power is interpolated on the convection grid in the NS3D layer). Concerning the secondary services, one just fixes the RHT grid whereas another one is needed to stop RadMC3D.

2.2.4 Migration on the DEISA infrastructure and first improvements

The coupled code has been migrated on the DEISA infrastructure without great difficulties and the two 3D codes have been validated separately. As the convection code presents a very good scalability and a good flexibility to load-balance the 2 codes, no special work has been done in a first time; we focused our activity on the radiative code which is estimated to be the most time consuming. Concerning the coupling project, the RadMC3D had the disadvantage to be parallelized for shared memory architectures, consequently the numerical simulations would be limited by the number of processors inside one node. To give more flexibility we decided to parallelize the code for general architectures i.e. with a distributed memory approach.

The parallelization work was not particularly hard since the event sequences of photon bundles are independent. Nevertheless a particular attention has been paid to avoid duplicating part of the random series on different processes. This new parallelized version has been tested and validated.

Recently the first 3D coupled simulations have been achieved to validate the coupled application and to obtain the first 3D coupled results.

2.3 ***Conclusion and future works***

The results obtained in the 2D coupling confirm that the radiative heat transfers have an important impact on the fluid structure inside the cavity. To reduce the computation cost of the RHT code, a study on the coupling frequency has been achieved at $R_a = 10^9$ and seems to indicate that the coupling frequency can be lowered without altering much the quality of numerical results. Nevertheless, more statistics and computations are needed to validate it. Concerning the 3D simulations, the 3D coupled application is now ready to run on the DEISA infrastructure and the first simulations have been launched. We have mainly adapted the two coupled codes to provide more flexibility to allow a good load balancing between this two modules.

3. FOCUS project

<i>Title</i>	Full coupling between radiatiOn and Combustion for Unsteady Simulation (FOCUS).
<i>Scientific leader</i>	Olivier Gicquel, EM2C (Laboratoire d'Energetique Moléculaire et Mascroscopique, Combustion), Chatenay Malabry, France.
<i>Partner Laboratories</i>	CERFACS/IMFT (Institut de Mécanique des Fluides de Toulouse), Toulouse, France.

This summarizes all the different tasks achieved during the last six months in the FOCUS project. FOCUS was selected as a DECI project in 2005.

3.1 *Technical Improvement*

The pre-processing code used to initially convert the mesh from the AVBP format to the specific format used by the radiation code has been fully re-written. Originally the code did not take any advantage of the AVBP format and connectivity to build the radiation mesh used in DOMASIUM. The main advantage of this code was that any mesh using any format could be treated. But the drawback is that it takes lots of CPU time to build the new connectivity table. Previous developments have been focused on the parallelization of this code using OpenMP. But even when using 16 processors the CPU needed to convert a 3 millions nodes AVBP mesh remained too large, around 10 days.

Then a new code dedicated to the transfer of AVBP mesh to DOMASIUM has been written. This code takes advantage of the connectivity table provided in the AVBP files. The CPU time needed to convert a mesh from AVBP format to DOMASIUM standard is now about a few minutes on one processor. No further developments should be done on this code.

In order to improve the efficiency of DOMASIUM, the code structure has been changed. These changes are based on the resolution technique used to solve the RTE. In the present model the RTE is solved for n different directions. For each direction a specific pathway is used to describe the mesh. To have an exact solution, the RTE needs to be solved on each cell using this pathway. This leads to an inefficient use of the memory caches because variables are randomly stored in memory. Therefore new developments have been conducted. In the present version of DOMASIUM, before solving the RTE all the variables are reordered using the pathway. The improvement led to a speed up equal to four. Another advantage coming with this modification is the decreasing of the memory required during the simulation. It is then possible to use meshes which include up to 3 Million nodes.

3.2 *Gas turbine injector simulation*

The test case used for these simulations, a swirled gas turbine injector, is presented in Figure 4. The computed geometry is 85 cm long and 60 cm wide. The radiative source term is computed using the CK model to describe the radiative properties. The present simulations only take into account 32 bands for H₂O and CO₂ to limit the CPU time dedicated to DOMASIUM. Two different meshes have been performed, one including 2,300,000 cells (mesh 1) and a second one locally refined in the flame location zone which includes 2,800,000 cells (mesh 2). This second mesh leads to use lower flame

thickening factors (about 25 instead 70 in the first mesh) and gives us a better description of the flame dynamics.

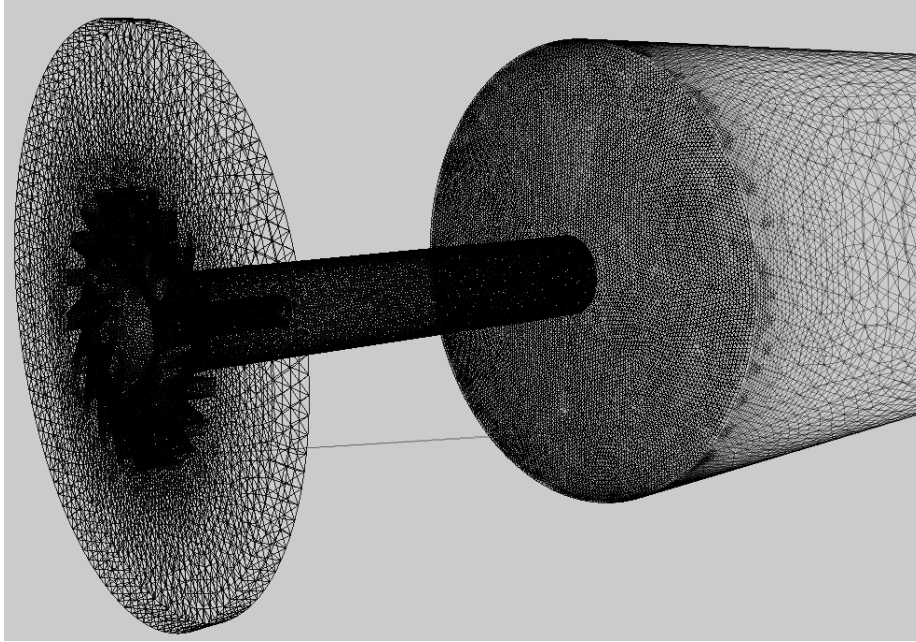


Figure 4: Mesh used to compute the gas turbine flame. It includes 2,300,000 cells (mesh 1 case). Simulations were performed using three different computing configurations:

- Case 1: The DOMASIUM version used is the one developed last year, without the remapping of the variable for each direction. The mesh is mesh 1. The total number of processors is equal to 116: 20 dedicated to LES (AVBP) and 96 to radiation computation (DOMASIUM).
- Case 2: The configuration is the same as in case 1 but the total number of processors was set equal to 348: 60 dedicated to LES (AVBP) and 288 to radiation (DOMASIUM).
- Case 3: In the present case, we used the last version of DOMASIUM, which includes the variable remapping for each direction. Computations were performed using 156 processors: 60 dedicated to LES (AVBP) and 96 to radiation (DOMASIUM).

For the 3 situations seen above, the CPU time of a time step for both codes are measured (t_{AVBP} , $t_{DOMASIUM}$) then the number of processors (t_{AVBP} and $t_{DOMASIUM}$) for each module are chosen so that:

$$\frac{t_{AVBP}}{NP_{AVBP}} = \frac{t_{DOMASIUM} \cdot F_{CPL}}{NP_{DOMASIUM}},$$

where F_{CPL} represents the coupling frequency ($F_{CPL} = 100$ for the 3 cases – see [13] and [17] for more information about coupling frequency).

At run time the processors activity ratio has been verified (greater than 95 %).

	AVBP	DOMASIUM	Coupled application
Case 1	20	96	116
Case 2	60	288	348
Case 3	60	96	156

Table 1: Load balancing between AVBP code and DOMASIUM code

Figure 5 presents an isocontour of the heat release coloured by the temperature. This isocontour is used to visualize the flame front position. One can see that in this configuration the flame is very compact and localized close to the injector. This behaviour is similar to the one observed in the experimental set-up.

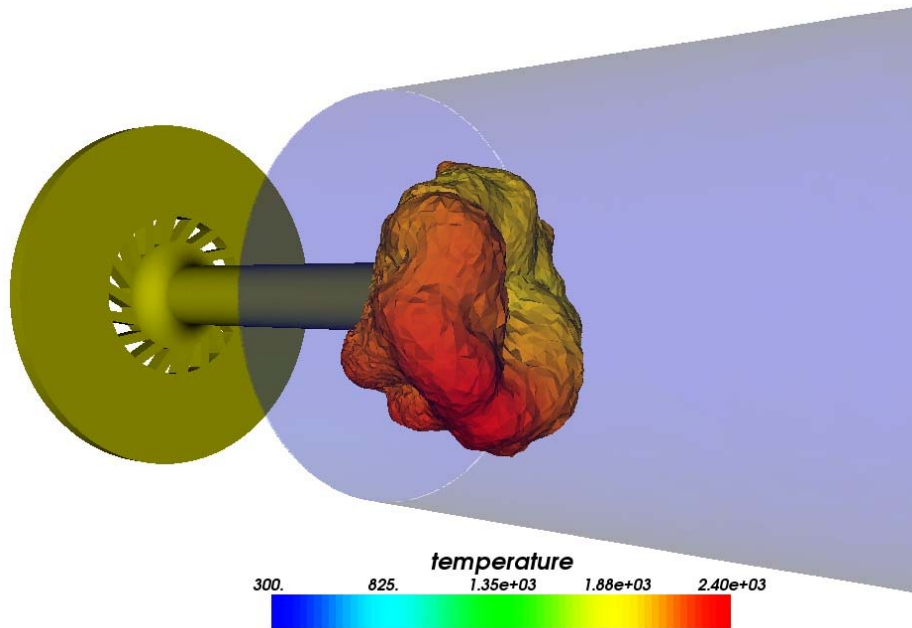


Figure 5: Isocontour of the heat release coloured by the temperature in a swirled injector of a gas turbine. This isocountour point out the flame shape.

Two 2D slices of the flame are presented in Figure 6. Figure 6-a presents the unsteady radiative power computed using DOMASIUM and sent through the CORBA framework to DOMASIUM while Figure 6-b presents the corresponding temperature unsteady field obtained using AVBP and used as an input by DOMASIUM.

Comparisons between these simulations, which take into account radiation effects and simulations performed without radiation, are now conducted. These results should be submitted to publication in 2007. A dedicated page on the EM2C web site presents the 3D project (see [9]).

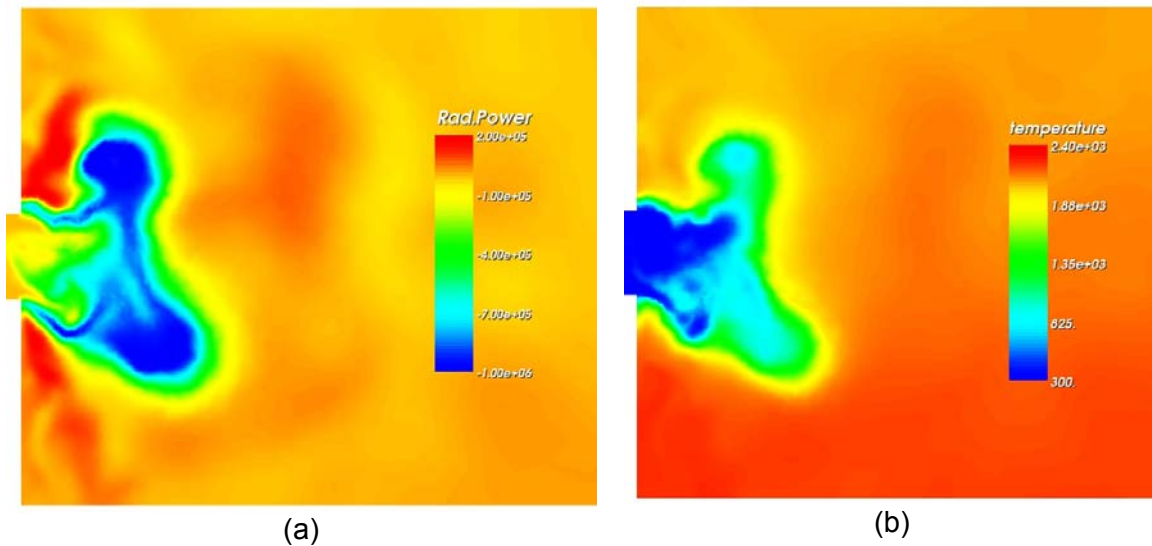


Figure 6: Two 2D slides presenting instantaneous fields of the radiative power (a) and the temperature (b).

3D simulations of a diedra flame holder device which is available at EM2C laboratory, are planned during the next months. Reference 3D simulations have already been performed without taking into account radiation module. The mesh needs 2,800,000 cells to cover the whole combustion chamber. The ultimate simulations should lead to the processor distribution: 120 dedicated to LES (AVBP) and 192 to radiation (DOMASIUM), i.e. 312 processors for the whole coupled application.

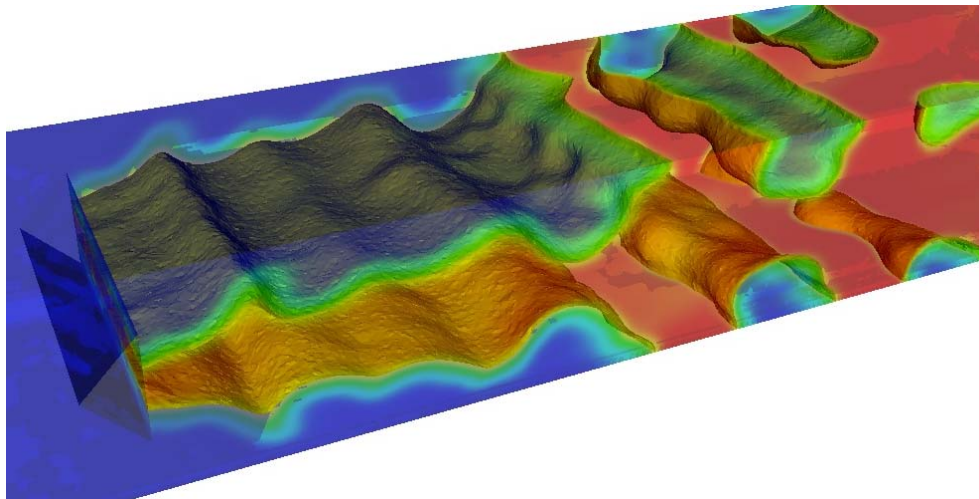


Figure 7: A 3D simulation of the diedra flame holder corresponding at an EM2C experimental setup.

3.3 **Conclusion and future work**

This period was mainly dedicated to start the DECI project. Two large configurations required a particular attention during their preparation and a continuous control has been provided to avoid wasting CPU resources.

As announced above, dielectric flame-holder simulations will complete the DECI project. The results obtained in the swirled injector configuration will be compared to available experimental measurements in order to quantify the impact of radiation in reacting flow numerical simulations. They will also be compared with previous results obtained in the 2D case (see [15], [16], [17] and [18]). These results will be described in the next deliverable.

4. The KOP3D project

<i>Title</i>	Kopplung 3D (KOP3D).
<i>Scientific leader</i>	Claus-Dieter Munz, IAG (Institut für Aerodynamik und Gasdynamik), Stuttgart University, Germany.
<i>Partner Laboratories</i>	Numerische Simulation und Auslegung eines instationär gepulsten magnetoplasmadynamischen Triebwerks für eine Mondsonde – Project of the "Landesstiftung Baden-Württemberg".

4.1 *Current scientific usage of KOP3D*

KOP3D is used for the simulation of aeroacoustic flows. The field of aeroacoustics gets a lot of attention currently, as it is getting feasible to calculate the source of the noise and its propagation within the flow at the same time. However, the direct numerical simulation of noise sources has different requirements than the wave propagation. KOP3D handles this by using a decomposition in subdomains, where the equations, timesteps and discretization methods may be adopted.

In total, KOP3D consists of three parts, the coupling, one flow solver for structured meshes and one solver for unstructured meshes. The coupling routines perform the spatial coupling as well as necessary subcycling for temporal coupling between the domains.

This coupling procedure enables the code to link even other different solvers together. For example in the working group at Institute for Aerodynamics and Gasdynamic (IAG) an external DNS code has been coupled with the KOP3D framework and currently it is investigated how the code may be coupled with the commercial CFX tool, to simulate the acoustics of an injection stream into a tube.

To simulate the effects in an aeroacoustic flow, high order schemes are necessary. KOP3D in its solver parts makes use of Discontinuous Galerkin schemes with arbitrary high order. Recently a new method was developed, to use reconstructed DG schemes and thereby allowing to span the polynomials over an arbitrary stencil.

This enables the use of a totally new class of schemes, which can continuously transform from Discontinuous Galerkin to Finite Volume. With this approach it is possible to use FV schemes of arbitrary high order.

On the European Conference on Computational Fluid Dynamics ECCOMAS CFD 2006, Jens Utzmann [26] presented the coupling method used in KOP3D. The ADER-DG method is presented in [27].

4.2 *Necessary parallelization efforts*

The two flow solvers were already parallelized and could be run as stand alone programs. But the coupling routines in KOP3D were still mostly sequential. These remaining sequential parts of the overall program had to be parallelized in order to employ a complete parallel operation of the coupled domains. However this turned out to be more work than expected.

The data structures in the sequential parts were not usable for a distributed memory usage, as each domain took the data directly from its neighbours to calculate the needed values on its own. This had to be changed to a model, where no direct access to the memory of the neighbour domains is necessary.

In the newly implemented routines, the domains only announce which values they need, and the neighbour calculates and communicates only those values over MPI.

Additionally some adjustments to the solvers themselves were necessary to enable them working within the parallel KOP.

4.3 *Considerations on shared memory usage with OpenMP*

We considered using an OpenMP parallelization within each domain. But meanwhile analysis of other codes on the machines deployed at the HLRS showed only small advantages which could be achieved only in special configurations. The usage of OpenMP and MPI would also increase the parallelization overhead and the complexity of the overall program. Because of the restriction of OpenMP to the shared memory architecture, it would still be necessary to use MPI within each subdomain in order to be able to distribute the domain over more than one node.

However, the parallelization within a single subdomain reduces the problem size for each processor and may result in a performance loss on machines with large vector registers like the NEC-SX8. It might be possible to partially recover this loss by using a hybrid parallelization, but the expected gains are quite low, so a further analysis is postponed.

4.4 *Parallel operation and load balancing concepts*

We ran the fully parallelized KOP3D on the high performance computing infrastructure at the HLRS site and validated the parallel implementation. We then investigated two load balancing concepts.

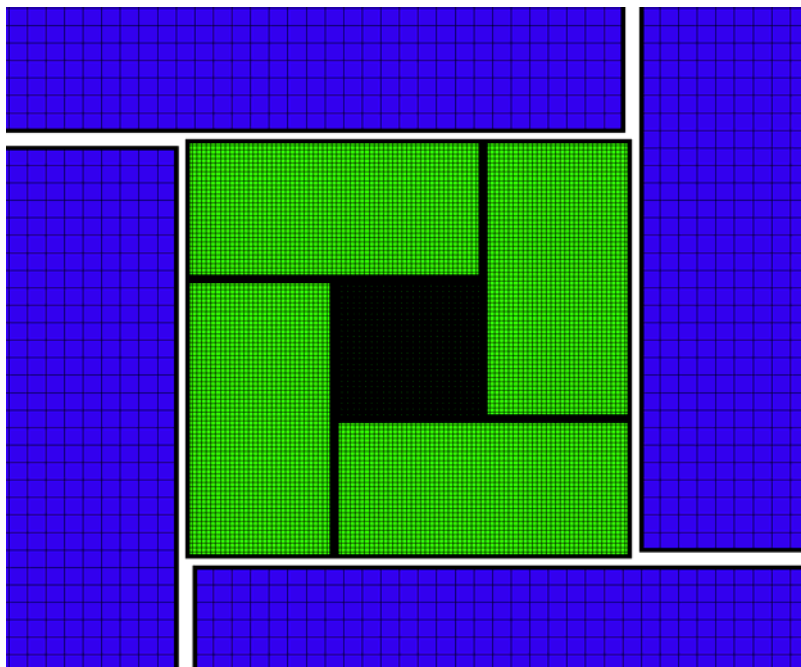


Figure 8: On the green domains in the middle the nonlinear Euler equations are solved, on the outer ones in blue the linearized equations. In the center domain (in dark), nonlinear Euler equations are solved with a very high resolution.

4.4.1 *Test case with structured domains*

In the first runs of the parallel KOP3D on the HLRS SX8, we used a test case with structured domains only, to validate the correctness of the parallel coupling. This test case is the corotating vortex pair from [28]. In the center of the computational area, two vortices are rotating around each other and thereby generate noise. The computational area is divided into 9 sub domains, as shown in **Figure 8**.

The nonlinear Euler equations are solved on the center domain with a very high resolution and on those surrounding it. In the 4 domains on the outer ring, which simulate the far field the linearized Euler equations are solved. Thus in this example we already use the coupling of different equations.

In the corotating vortex test case introduced above the fine resolved domain in the center consumes about 90% of the calculation time, and we used the *all processes for all domains* approach here.

Some rewriting of the code was necessary in order to gain better performance on SX8.

For the structured linearized solver itself, a vectorization of about 98.92 % is reached by now, which leads to nearly 8 GFLOPs on a single process. However the performance of the nonlinear solver on the vector machine is not so good. The vectorization for the main working routine here was only around 80%, and we raised this to the same level that is achieved in the linearized routine.

The memory usage increases for higher order schemes. By the parallelization and adaptation to the high performance computing infrastructure achieved in this JRA context, it is now possible to solve problems with very high orders, which could not be solved before because of their memory requirements.

4.4.2 *Test case with unstructured mesh surrounded by structured meshes*

For our first operational tests with an unstructured domain surrounded by structured domains, we used a benchmark problem given in [29]. In this problem the scattering of a time harmonic plane sinusoidal acoustic pressure fluctuation incident on a cylinder with perfectly reflecting walls is to be computed. The whole computation area is decomposed into a unstructured domain around the cylinder and 4 structured domains in a ring around the unstructured domain. This decomposition is shown in Figure 9.

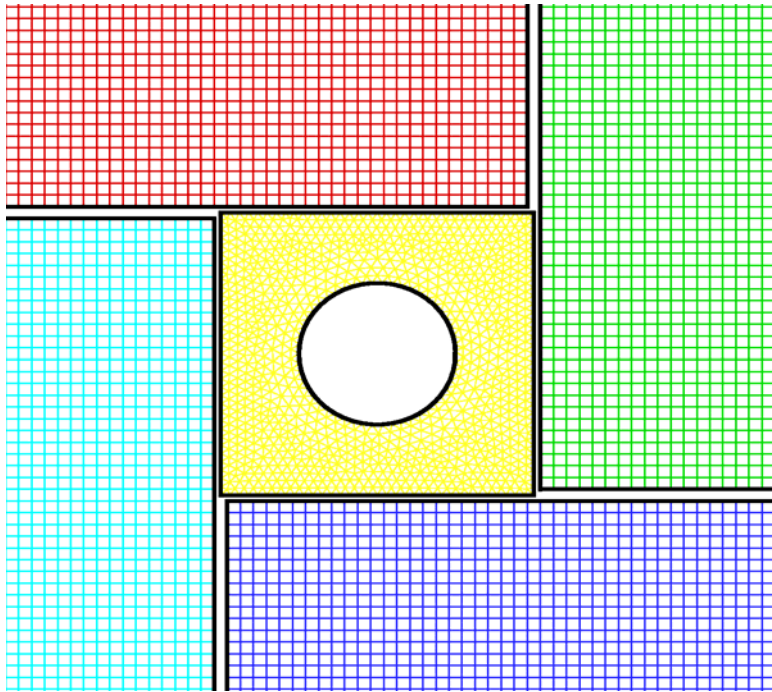


Figure 9: An unstructured domain (yellow mesh) around the cylinder surrounded by a ring of structured domains.

The vectorization of the unstructured computation cannot be pushed as far as that of the structured one, the main calculation routines are here somewhere around 60%. So it is one goal to exploit the possibilities of the different architectures for the different domains. For our test case, the SX8 needed for the unstructured domain about 16% more time than on a scalar machine, whereas for the structured domains it needed about 24% less time.

We are in the progress of exploiting these architecture specific properties by using the PACX-MPI infrastructure, but we still need to reduce the overhead of the coupling further to see real gains here. Especially a good balancing to avoid idle times is necessary along a well suited distribution fitting the processes to the domains.

4.5 Load balancing analyses

Two approaches on distributing the domains on the processors have been investigated. To get a good load balancing the simplest possibility is to give each processor an equal part of each domain (all for all). Thus the computational costs are the same within each subdomain. However this leads to a lot of communication as these results in “subdomains x number of processors” MPI sections, which have to communicate with each other. So the second method used for distributing the subdomains is to configure the distribution before calculation in a way that communication interfaces coincide with the coupling surfaces between the subdomains. The interaction on these subdomain boundaries is necessary anyway and the coupling is less strong than within a single domain, as due to the subcycling capability of KOP3D one domain may do more than one timestep, before communication is necessary again. Whereas processes on the same domain have to exchange data within each timestep.

Additionally, the SX8 is especially well suited for large problems, as it has long vector registers. If the domains are subdivided by all available processes, the problem size within each section is decreased rather fast.

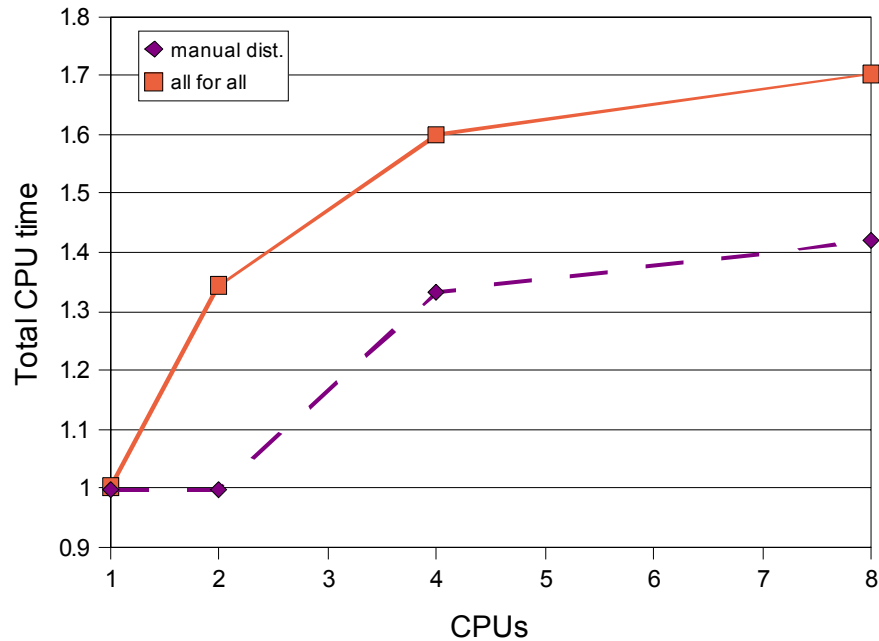


Figure 10: Comparison of the two load distributing methods.

In this configuration we tested the distribution of processes along the given interfaces, as far as possible. In the case of 2 processors, one calculates the unstructured domain around the cylinder and the other one calculates the 4 structured domains. When 4 processors are available, 2 of them share the unstructured domain, and the remaining ones take each 2 structured domains. Finally if we use 8 processes, 4 of them take each one structured domain and the unstructured domain is shared by the other 4 domains.

In Figure 10 it is shown that communication overhead can be avoided by taking advantage of the natural decomposition within KOP. However this adaptation is still made manually, as the parallel KOP has not yet a data structure, which would allow us to distribute the domains in more automated and better adapted way. This is an improvement we need to implement to allow dynamic load balancing, too.

Even so, some optimizations to the coupling routines have been made; this is still the part, that mostly drives the overhead in the parallel program. In the following figures (Figure 11) the parts of the CPU time used on the several parts is shown.

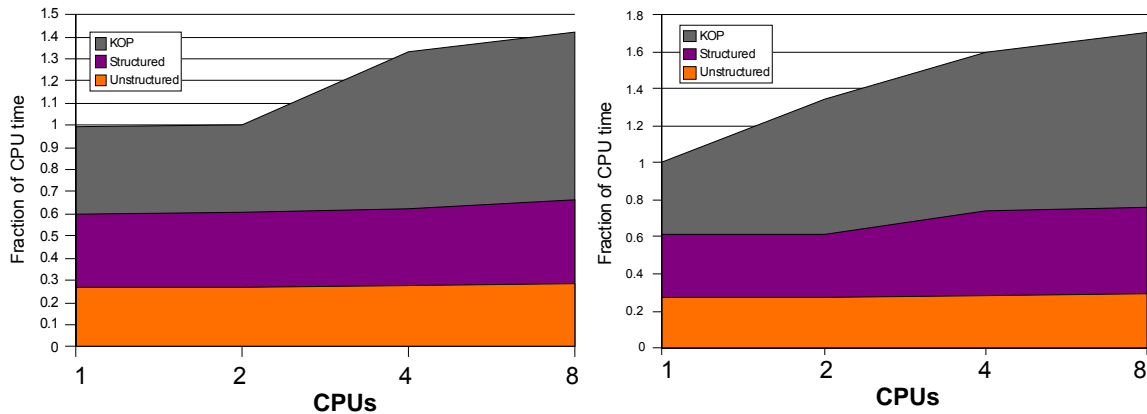


Figure 11: Fractions of the CPU time spent on the several parts of the program. The manually distribution (left figure) and the distribution of all processes on all domains (right figure) are shown

The time needed for the coupling routines increases with the number of CPUs, that have to exchange large datasets. This can be observed for the manually distributed processes, where, for 2 processes all the structured domains with large interfaces are within the same CPU. For more CPUs, large datasets have to be exchanged at the interfaces and the time for coupling increases. With equal distribution of all domains on all processes, the coupling is still the most growing part, but the MPI communication within the subdomains themselves increases the overhead additionally. So the simple distribution of all domains to all processes may be sufficient for a small number of CPUs, but taking advantage of the given natural subdivisions of KOP results in a notable performance gain.

4.6 Conclusion and future work

KOP3D presents now several levels of parallelism which enable to distributed the work more easily and which provide more conveniences to load-balance the whole application.

Our main goals are now to optimize the coupling with respect to communication in the parallel high performance computing environment, and to implement some dynamic load balancing.

5. Conclusion

Several important achievements have been done during the last six months. The DECI project FOCUS has already performed 2 large mesh configurations of the coupled Combustion/Radiation application. Concerning KOP3D, a deep analysis has been made about the coupled application load-balancing. This study has led to carry out several solutions to improve the performances of the coupling part and to facilitate the application load balancing. Nevertheless an optimization work is still needed to reduce the coupling overhead. The Natural Convection project has shown in this document the physical impact of the radiative transfers on the 2D convection process. With the work done in this JRA, this project benefits now of a coupled 3D tool dedicated to large physical configurations.

The next report is going to focus on the last achievements and, more particularly, on describing the results obtained for the three projects.

6. References and Applicable Documents

- [1] <http://www.deisa.org>
- [2] <http://www.omg.org>
- [3] <http://omniorb.sourceforge.net/>
- [4] <http://unicore.sourceforge.net/>
- [5] <http://www.eurogrid.org/>
- [6] <http://www.limsi.fr/>
- [7] <http://www.let.ensma.fr/>
- [8] <http://www.em2c.ecp.fr/>
- [9] <http://www.em2c.ecp.fr/ACTIVITES/NUMERIQUE/CORAYL/corayl.html>
- [10] <http://www.cerfacs.fr>
- [11] Deliverable D-JRA6-1 — *Grid-enabled simulation codes: status report of first release* — October 2004.
- [12] Deliverable D-JRA6-2 — *Production operation of distributed simulation codes: status report* — April 2005.
- [13] Deliverable D-JRA6-3 — *Production operation of distributed simulation codes: status report* — October 2005.
- [14] Deliverable D-JRA6-4 — *Grid enabling the second set of projects: status report of the first release* — April 2006.
- [15] M. Lecanu, S. Ducruix, O. Gicquel, E. Iacona, D. Girou, J.M. Dupays and D. Veynante — *Numerical simulation of turbulent combustion including pollutant formation and radiative heat transfers using coupled codes* — Tenth International Conference on Numerical Combustion, Sedona, Arizona, U.S.A on May 9-11 2004 organised by the SIAM (Society for Industrial and Applied Mathematics)
- [16] M. Lecanu — *Couplages multi-physiques : combustion turbulente, rayonnement et cinétique chimique* — PhD thesis (in French), EM2C laboratory, Ecole Centrale de Paris (February 2005)
- [17] R. Gonçalves dos Santos, M. Lecanu, S. Ducruix, O. Gicquel, E. Iacona, and D. Veynante, – *Large Eddy Simulations of combustion / radiative heat transfers coupling using the specialized communication language CORBA* – The Cyprus International Symposium on Complex Effects in Large Eddy Simulations (CY-LES 2005) – Limassol, Cyprus (September 2005).

-
- [18] R. Goncalves dos Santos, S. Ducruix, O. Gicquel, E. Iacona, and D. Veynante — *Large Eddy Simulations of Turbulent Combustion Including Radiative Heat Transfers using Specialized Communication Language* — 11th International Conference on Numerical Combustion, Granada, Spain (2006).
- [19] J. Salat, S. Xin, P. Joubert, A. Sergent, F. Penot et P. Le Quéré — *Experimental and Numerical Investigation of Turbulent Natural Convection in a Large Air-filled Cavity* — Int. J. of Heat and Fluid Flows, volume 25(5), pp 824-832 (2004).
- [20] H. Wang, S. Xin et P. Le Quéré — *Etude numérique du couplage de la convection naturelle avec le rayonnement de surfaces en cavité carrée remplie d'air* — C.R. Mécanique (in French), volume 334, pp 48-57 (2006).
- [21] R. Siegel & J.R. Howell — *Thermal radiation heat transfer* — Hemisphere, Taylor and Francis, 3rd Edition (1992).
- [22] M.F. Modest — *Radiative heat transfer* — McGraw-Hill (1993).
- [23] T.H. Gogel, A. Sedghinasab and D.R. Keefer — *Radiation transfer computation in cylindrical arc columns using a Monte Carlo method* — Journal of Quantitative Spectroscopy and Radiative Transfer, vol. 52, n°2, pp. 179-194 (1994).
- [24] C. Deron, P. Rivière, M.Y. Perrin and A. Soufiani — *Couples radiation, conduction and Joule heating in argon thermal plasmas* — Journal of Thermophysics and Heat Transfer, vol. 20, n°2, pp. 211-219 (2006).
- [25] J.R. Howell — Application of Monte Carlo to heat transfer problems — Advances in Heat Transfer, vol. 5, pp. 1-54 (1992).
- [26] C.D. Munz, and J. Uitzmann — *Heterogeneous Domain Decomposition for the Efficient Simulation of Wave Propagation in Complex Domains* — ECCOMAS CFD 2006, Egmond aan Zee, The Netherlands, (September 2006).
- [27] M. Dumbser and C.-D. Munz — *ADER discontinuous Galerkin schemes for aeroacoustics* — Comptes Rendus Mécanique, vol. 333, issue 9, pp. 683-687 (2005).
- [28] T. Schwartzkopff — *Finite-Volumen Verfahren hoher Ordnung und heterogene Gebietszerlegung für die numerische Aeroakustik* — Dissertation, Stuttgart (2004).
- [29] C._D. Munz et. al. — *Heterogeneous Domain Decomposition for CAA* — 11th AIAA/CEAS Aeroacoustics Conference, Monterey, California (May 2005).

7. Document Amendment Procedure

8. List of Acronyms and Abbreviations

AVBP	CFD code for numerical simulation of unsteady turbulence for reactive flows (developed by the CERFACS).
CFD	Computational Fluid Dynamics.
CFL	Courant-Friedrichs-Lewy condition. Time step constrain to obtain a correct convergence to solve partial differential equations.
CORBA	Common Object Request Broker Architecture is the OMG's specification which defines the middleware to allow remote computer applications to work together over networks.
DG	Discontinuous Galerkin.
DNS	Direct Numerical Simulation.
DOM	Discrete Ordinate Method.
EM2C	Laboratoire d'Energetique Moléculaire et Mascroscopique, Combustion at Chatenay Malabry, France.
FV(M)	Finite Volume (Method).
IAG	Institut für Aerodynamik und Gasdynamik, Stuttgart University, Germany.
LES	Large Eddy Simulation.
LET	Laboratoire d'Etudes Thermiques at Poitiers, France.
LIMSI	Laboratoire d'Informatique pour la Mécanique et les Sciences de l'Ingénieur at Orsay, France.
OMG	The Object Management Group is a consortium that produces and maintains computer industry specifications for interoperable enterprise applications. The other well-known specifications are UML (Unified Modelling Language) and MDA (Model Driven Architecture).
OpenMP	Open Multi Processing.
PACX-MPI	Parallel Computer eXtension MPI.
Mtoe	Mega-ton of oil equivalent.
RMS	Root Mean Square.
RTE	Radiative Transfer Equation.
RHT	Radiative Heat Transfer.